Simple electronic analog of a Josephson junction

R. W. Henry
Department of Engineering and Applied Science, Becton Center, Yale University, New Haven, Connecticut 06520 and Physics Department, Bucknell University, Lewisburg, Pennsylvania 17837[a]

D. E. Prober
Department of Engineering and Applied Science, Becton Center, Yale University, New Haven, Connecticut 06520

A. Davidson
IBM Watson Research Center, Yorktown Heights, New York 10598
(Received 4 September 1980; accepted 22 January 1981)

We describe an electronic analog of a resistively shunted Josephson junction in which the quantum phase difference of a real junction is represented by the phase difference between two oscillators, each running at approximately 100 kHz. Only three integrated circuits and an external reference oscillator are required. The circuit operates on a time scale approximately 10^9 times slower than a typical real junction and allows easy visualization of the time-dependent quantum phenomena of the ac Josephson effect. Characteristic current–voltage curves and waveforms obtained with the analog are shown for the cases of dc and dc plus ac current bias, and for the sudden reduction of the critical current in a current-fed, resistively loaded junction, which models a magnetically switched Josephson computer element. Other applications of the analog are discussed.

I. INTRODUCTION

It has been nearly two decades since Brian Josephson's Nobel Prize winning prediction[1] of the effects that bear his name, and their subsequent experimental verification.[2,3] Since that time the Josephson effects have come to be recognized as a most convincing verification of quantum-mechanical tunneling and macroscopic quantum interference. In addition, they have led to extremely sensitive scientific instruments for measuring low-frequency voltages and magnetic fields, [4,5] have been employed as detectors for microwave and far-infrared radiation,[5] have provided an accuracy of 0.12 parts per million in the measurement of the ratio of Planck's constant to electronic charge,[6] and are on the verge of producing a major advance in the performance of large computers.[7]

While the equations describing the quantum-mechanical tunneling and interference in Josephson devices are readily derived,[8] the observable electrical *circuit* behavior of a Josephson junction device is not trivial because it is described by nonlinear differential equations. It is therefore useful, both as an aid to understanding and for predicting the engineering performance of real devices, to make models or analogs that mimic the behavior of Josephson junctions. Several such models, [9–14] both mechanical and electrical, have been described in the literature.

Mechanical models, usually involving pendulums, have the great advantage of actual visual representation of some of the variables on a time scale that is slow enough for the viewer to comprehend in real time. Spatially extended junctions and multiple junction circuits are also easily modeled. On the other hand, with mechanical models it is difficult to make quick and accurate measurements, to change the model parameters over wide ranges, or to model the interaction of ac currents or voltages with the junction. Furthermore, good mechanical models can involve a considerable amount of machine shop work.

Electronic models provide an excellent complement to mechanical models. Interactions with time-varying applied currents or voltages can be easily simulated, and time-dependent and time-average behavior readily recorded. Moreover, measurements are quick and accurate and it is usually a trivial matter to change model parameters. The phase-locked-loop type of electronic model described here offers the additional advantages of simplicity of construction and use, and ease of adjustment. Furthermore, the model is quite accurate in its simulation of the Josephson equations. While the basic idea for this circuit and certain of the results obtained from it have appeared previously,[14] this is the first article to provide a complete description of a practical circuit, which is in fact simpler to implement than the circuit originally proposed.[14] In addition, the circuit to be described can be extended to construct single and double junction SQUIDs (Superconducting Quantum Interference Devices). That work is presented in a separate article.[15]

The circuit and experiments described here can be an effective supplement to a senior-level or first-year graduate experiment on the properties of real Josephson devices.[16] The analog may also be used profitably by itself, especially if the circuit functions of the analog and their relation to important laboratory instruments such as the lock-in amplifier are discussed. Alternatively, for electrical engineers the rich behavior of the nonlinear second-order circuit element may be treated in detail.[15] Since Josephson devices are finding increasing application as sensors in the physical and biological sciences, and as high-speed digital circuit elements in the electrical sciences, the incorporation of some type of Josephson-effect experiment into the laboratory curriculum seems especially appropriate. The electronic analog opens up this opportunity even to laboratories where liquid helium is not available.

It is the purpose of this article to discuss experiments with the analog that emphasize aspects of Josephson-effect quantum-mechanical tunneling. A number of excellent introductory treatments have previously been given on the

 0002-9505/81/111035-12$00.50

theory of the Josephson effects,[8,10] of quantum interference,[8,9] and of the mechanical analog.[9–11] We refer the reader to these discussions where appropriate. Finally, excellent discussions[8,9] and a laboratory experiment[16] on fluxoid quantization have been given by other authors. While we do not treat this subject here, it is possible to model fluxoid quantization[15] with the electronic analog to be described.

II. JOSEPHSON EQUATIONS AND THE RESISTIVELY SHUNTED JUNCTION (RSJ) MODEL

The unique electrical behavior of Josephson devices is a consequence of the fact, shown theoretically by Bardeen, Cooper, and Schrieffer,[17] that the electrons in a superconductor condense, via mutual interactions with the crystal lattice, into Cooper pairs of charge $2e$ and spin 0.[18] Because they act like bosons, many such pairs can occupy the same quantum state; indeed, in the absence of thermal excitations, (i.e., at $T = 0$ K), *all* of the electrons are in a single quantum pair state. This quantum state of the $\sim 10^{22}$ electrons can for many purposes be represented by a conventional single-particle wave function $\psi(\mathbf{r},t)$. (See Ref. 4, Chaps. 4 and 6.) Thus in an isolated superconductor the time-dependent wave function that describes a spatially uniform *stationary* state of energy E can be written as $\psi = |\psi| e^{i[\theta(0) - Et/\hbar]}$, with $\theta(0)$ the phase at time $t = 0$, and $\hbar = h/2\pi$, h being Planck's constant. Josephson showed[8] that when two superconductors, with stationary wave functions $|\psi_1| e^{i[\theta_1(0) - E_1 t/\hbar]}$ and $|\psi_2| e^{i[\theta_2(0) - E_2 t/\hbar]}$ are separated by an insulating barrier of thickness on the order of 20 Å, a current $I_s(t)$ of Cooper pairs can tunnel across the junction. (The Josephson coupling also reduces the energies E_1 and E_2 relative to their values when the two superconductors are well separated.[18]) Josephson further showed that for these stationary states the tunnel current of paired electrons depends on the quantum phase *difference*

$$\theta(t) \equiv \theta_2(t) - \theta_1(t) = (E_1 - E_2)t/\hbar + \theta_0,$$

according to

$$I_s(t) = I_c \sin\theta(t). \tag{1}$$

Here I_c is the maximum or critical supercurrent and is a geometry- and material-dependent constant; θ_0 is the phase difference at $t = 0$, $\theta_2(0) - \theta_1(0)$. Particularly clear derivations of Eq. (1) are given in Ref. 8, and by Rochlin and Hansma, Ref. 10.

The time rate of change of the phase difference $d\theta/dt$ is given in general by $(E_1 - E_2)/\hbar$. If a voltage $V(t)$ exists across the junction (with V defined as the potential of side 1 with respect to side 2), then $E_1 - E_2 = 2\,\text{eV}$. For the general case of a *time-dependent* voltage $V(t)$, $\theta(t)$ must be defined as

$$\theta(t) = \frac{2e}{\hbar}\int_0^t V(t')dt' + \theta_0,$$

and for either a constant or time-dependent junction voltage

$$\frac{d\theta}{dt} = \frac{2eV(t)}{\hbar}. \tag{2}$$

Equations (1) and (2) provide the basic description of the supercurrent flow in Josephson devices. While Eq. (1) was derived by Josephson for the case of tunneling through a potential barrier as in a superconductor–insulator–superconductor tunnel junction [Fig. 1(a)] a wide variety of other weak-link superconducting stuctures are also found to obey that equation.[4,5] These other structures include the metallic point contact and its thin-film analog, the microbridge [see Figs. 1(b) and 1(c)] and the superconductor–nonsuperconducting-metal–superconductor junction. Point contacts and microbridges utilize a *physical* constriction to confine the change in quantum-mechanical phase to a small region. *Weak coupling* between two superconductors, whether achieved by a physical or a material constriction, is the essential requirement for occurrence of the Josephson effect.

In addition to the supercurrent of Cooper pairs, a normal electron current of unpaired electrons flows through the junction in response to a voltage across the junction. This current is sometimes called a quasiparticle current. Within the two-fluid model of superconductivity[4] the pair current and the quasiparticle current are considered to be independent.

For point contacts and microbridges the normal current channel can be adequately modeled by an ohmic resistor in parallel with the supercurrent channel, whose behavior is described by Eqs. (1) and (2). For insulator (usually oxide)–barrier tunnel junctions the normal current is a nonlinear function of the junction voltage. The nonlinear quasiparticle conductance of such tunnel junctions rises sharply at a voltage corresponding to the energy gap for breaking pairs and creating unpaired electrons (quasiparticles). This structure in the conductance due to the energy gap was predicted and studied first by Ivar Giaever,[19] who shared the Nobel Prize in 1973 with Josephson and Leo Esaki. In this paper the normal current channel will be modeled by an *ohmic resistor* R. The resulting model is called the *resistively shunted junction* (RSJ) *model*,[20] and is most appropriate for point contacts and microbridges.[21] However, the RSJ model is also qualitatively useful for describing the behavior of insulator–barrier tunnel junctions.

To complete the circuit model of a Josephson junction one must include the displacement current due to charging and discharging the inevitable shunt capacitance across the junction structure. For oxide–barrier tunnel junctions, the capacitance is due to the parallel-plate electrode structure with a $\sim$20-Å separation, and is usually significant. The capacitance of point contacts and microbridges is usually small enough to be neglected.[21]

The complete RSJ model, including the capacitance, is shown in Fig. 2(a). The total current $I(t)$ through the junction is given by

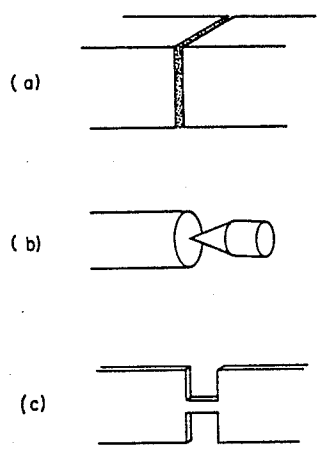

Fig. 1. Three types of weak links connecting bulk superconductors: (a) insulator-barrier tunnel junction, (b) point contact, (c) microbridge. Tunnel junctions and microbridges are usually made by thin-film techniques. The resistively shunted junction (RSJ) model is most appropriate for point contacts and microbridges.

$$I(t) = I_c \sin\theta(t) + \frac{V(t)}{R} + C\frac{dV(t)}{dt}. \quad (3)$$

In a real junction these three currents are not independently accessible, though they are accessible in the electronic analog.

The voltage in Eq. (3) may be eliminated with the help of Eq. (2) to arrive at the nonlinear second-order differential equation that describes the junction dynamics:

$$I(t) = I_c \sin\theta(t) + \frac{\hbar}{2eR}\frac{d\theta}{dt} + \frac{\hbar C}{2e}\frac{d^2\theta}{dt^2}. \quad (4)$$

This equation has the same form as the equation of motion of a simple pendulum of mass m and length l displaced from the vertical by angle θ. In the pendulum model, the analogous equation is

$$\tau = mgl\sin\theta + D\frac{d\theta}{dt} + M\frac{d^2\theta}{dt^2},$$

where τ is the total externally applied torque, $mgl\sin\theta$ represents the gravitational restoring torque, $D\,d\theta/dt$ represents a damping torque proportional to velocity, and $M\,d^2\theta/dt^2$ is the rate of change of angular momentum about the point of suspension. Since a flywheel can be rigidly coupled to the pendulum,[9,11] the total moment of inertia M can be greater than the moment of inertia of the pendulum mass, ml^2. It is important to note that in the pendulum analog it is difficult to change the moment of inertia, the damping constant and the gravitational torque independently. On the other hand, in the electronic model each term in Eq. (4) depends on an independently adjustable quantity (I_c,R,C). An example in which this is important, where a sudden change of the critical current I_c is used to simulate a computer switch, is given later. An analogous change in the gravitational torque in the case of the pendulum would be difficult to achieve. With the electronic analog it is also possible to simulate the nonlinear quasiparticle conductance of an insulator–barrier tunnel junction by using a nonlinear resistor.[15]

III. ELECTRONIC MODEL OF A JOSEPHSON JUNCTION

Three types of circuits have been proposed to simulate the behavior described by Eqs. (1) and (2). The first type[12] integrates the junction voltage with respect to time to obtain a voltage that represents the phase angle $\theta(t)$, and a nonlinear function generator produces the sine of $\theta(t)$. Because $\theta(t)$ could become large without bound, each time the magnitude of the angle voltage reaches a value corresponding to 2π a comparator is triggered that resets the angle voltage to zero.

The second type[13] of circuit uses feedback to enforce the equalities

$$kV(t)\cos\theta = \frac{d}{dt}(\sin\theta) = \frac{d\theta}{dt}\cos\theta$$

and

$$-kV(t)\sin\theta = \frac{d}{dt}(\cos\theta) = -\frac{d\theta}{dt}\sin\theta,$$

along with an explicit, circuit-imposed constraint $\sin^2\theta + \cos^2\theta = 1$ to obtain the relations in Eqs. (1) and (2). An analog computer is usually employed in this second type of circuit. Integrators and multipliers are used to generate voltages proportional to $\sin\theta$, $\cos\theta$, $\sin^2\theta$, and $\cos^2\theta$, and a voltage-to-current converter generates a current $I_c\sin\theta$. This method requires an auxiliary correction circuit to prevent the accumulation of errors due to imperfect integrators.

The third type of circuit, a modified phase-locked loop, was first proposed by Bak and Pederson.[14] Our circuit is of this general type. A block diagram of our circuit appears in Fig. 2(b). The phase difference $\theta(t)$ in the real junction is represented in the electronic analog by the phase difference between the waves produced by two oscillators, one a sinusoidal reference oscillator running at a fixed angular frequency ω_0. The other is a voltage-controlled oscillator (VCO) with a square-wave output whose instantaneous angular frequency $d\theta_1/dt$ deviates from ω_0 by an amount proportional to $V(t)$, the input voltage to the VCO, so that

$$\frac{d\theta_1}{dt} = \omega_0 + kV(t). \quad (5)$$

If we assume for the moment that the VCO output wave is sinusoidal rather than square, the VCO output voltage can be written

$$V_{\rm VCO}(t) = V_1\sin\theta_1(t), \quad (6)$$

where V_1 is a constant and

$$\theta_1(t) = \theta_0 + \int_0^t \frac{d\theta_1(t')}{dt'}dt' = \theta_0 + \omega_0 t + \int_0^t kV(t')dt' \quad (7)$$

with θ_0 the phase at $t=0$. The angular frequency ω_0 is much larger than $|kV(t)|$ so that the fractional difference between the VCO and reference oscillator frequencies is always small. The mixer multiplies the VCO output by the reference signal, which we write as

$$V_{\rm REF}(t) = V_2\cos\omega_0 t \quad (8)$$

to obtain

$$V_{\rm Mixer}(t) = \alpha V_1 V_2\sin\theta_1(t)\cos\omega_0 t, \quad (9)$$

where α is a proportionality constant. Equation (9) may be rewritten with the help of a trigonometric identity to obtain

$$V_{\rm Mixer}(t) = (\alpha V_1 V_2/2)\{\sin[\theta_1(t) + \omega_0 t] + \sin[\theta_1(t) - \omega_0 t]\}, \quad (10)$$

and substitution for $\theta_1(t)$ from Eq. (7) results in

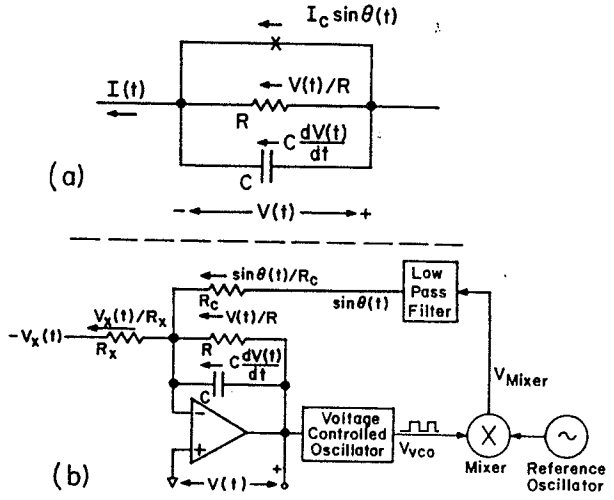

Fig. 2. Models of Josephson junctions. (a) Resistively shunted junction (RSJ) model, (b) electronic analog of the circuit in (a) showing how a current proportional to $\sin\theta$ is obtained. See text for explanation.

$$V_{\text{Mixer}}(t) = \frac{\alpha V_1 V_2}{2}\sin\left(2\omega_0 t + k\int_0^t V(t')dt' + \theta_0\right) + \frac{\alpha V_1 V_2}{2}\sin\left(k\int_0^t V(t')dt' + \theta_0\right). \quad (11)$$

The first term on the right-hand side represents a wave of instantaneous angular frequency equal to $2\omega_0 + kV(t)$, which for a time-varying $V(t)$ consists of waves of many different angular frequencies near $2\omega_0$. These high-frequency components are all strongly attenuated by the low-pass filter. The second term on the right-hand side of Eq. (11) represents a wave of instantaneous phase

$$\theta(t) = \int_0^t kV(t')dt' + \theta_0 \quad (12)$$

or instantaneous angular frequency

$$\frac{d\theta}{dt} = kV(t) \quad (13)$$

as required by Eq. (2). Because all significant Fourier components of $kV(t)$ are below the cut-off frequency of the low-pass filter, the second wave passes through the filter to produce a voltage proportional to $\sin\theta(t)$. In our circuit the proportionality constant $\alpha V_1 V_2/2$ is set at 1 V so that the voltage at the output of the low-pass filter is numerically equal to $\sin\theta(t)$.

The VCO output signal is actually a square wave, which for the general case of a time-varying $V(t)$ has components near the fundamental angular frequency ω_0 as well as at higher harmonics near angular frequencies $3\omega_0$, $5\omega_0$, etc. [We assume here again that $|kV(t)| \ll \omega_0$.] When these higher harmonics are multiplied by the reference sinusoid at angular frequency ω_0 the product at the mixer output contains high-frequency signals with angular frequencies near $2\omega_0$, $4\omega_0$, $6\omega_0$, etc. These signals are all blocked by the low-pass filter so our basic result, that the low-pass-filter output wave is proportional to $\sin\theta(t)$, is still valid.

Now that we have shown how a wave $\sin\theta(t)$ is produced, we show why the entire circuit of Fig. 2(b) is an analog of the RSJ model of Fig. 2(a). Using the standard virtual ground approximation[23] that the inverting input of the op-amp is at ground potential, we equate to zero the sum of the currents flowing toward the negative input. Thus

$$C\frac{dV(t)}{dt} + \frac{V(t)}{R} + \frac{\sin\theta}{R_c} - \frac{V_x(t)}{R_x} = 0, \quad (14)$$

with $V(t)$ the voltage at the output of the op-amp. [In obtaining Eq. (14) we have neglected any bias current drawn by the op-amp itself. For the type 741 op-amp shown, this bias current is a fraction of a microamp, at least two orders of magnitude smaller than the typical currents that flow through R, R_c, and R_x.] This op-amp feedback circuit accomplishes at once the required voltage-to-current conversion and current summation, and is thus a considerable improvement over the circuit configuration proposed by Bak.[14]

Next we use Eq. (13) to rewrite Eq. (14) in the form

$$\frac{C}{k}\frac{d^2\theta}{dt^2} + \frac{1}{kR}\frac{d\theta}{dt} + \frac{\sin\theta}{R_c} = \frac{V_x(t)}{R_x}. \quad (15)$$

This equation has the same form as Eq. (4) provided we make the identifications

$$I_c \rightarrow \frac{1}{R_c}, \quad I(t) \rightarrow \frac{V_x(t)}{R_x}, \quad \text{and} \quad k \rightarrow 2e/\hbar.$$

The entire circuit of Fig. 2(b) may be thought of as a phase-locked loop. To see this, consider the special case in which $C = 0$ and $V_x(t) = 0$, so that Eq. (15) reduces to

$$\frac{d\theta}{dt} = -\frac{kR}{R_c}\sin\theta.$$

If θ is slightly positive, so that $\sin\theta$ is positive, then $d\theta/dt$ is negative and θ is driven toward 0. Similarly, a small deviation of θ in the negative direction is corrected toward zero by a positive $d\theta/dt$. Consequently, the circuit maintains a stable phase of $\theta = 0$. By a similar argument, the apparent solution $\theta = \pi$ is unstable, and the phase will change until it reaches the stable value $\theta = 0$.

The actual circuit, Fig. 3, contains just three integrated circuits in addition to the reference oscillator. The choice of components was determined by tradeoffs between simplicity and accuracy. For example, the VCO should ideally have a precisely linear frequency-versus-voltage characteristic and no frequency drift or jitter when its input voltage is held constant. We tested three types of integrated circuit VCO's: the VCO in the CMOS-type 4046 micropower phase-locked loop, the Intersil 8038 waveform generator, and the Analog Devices AD 537 JD.[24] The long-term (many minutes) frequency drift of the AD 537 was about $\pm$ 1 part in 10^5 and the short-term ($\sim$10 msec) jitter, measured as fluctuations in the duration of 1000 cycles of oscil-

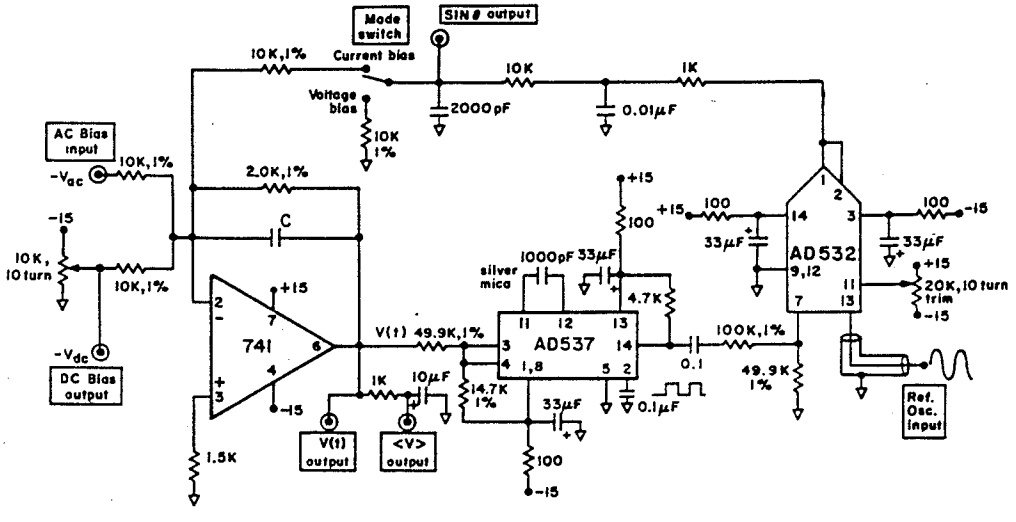

Fig. 3. Detailed circuit diagram of the electronic analog of Fig. 2(b). Provisions are made for either voltage biasing the supercurrent channel or current biasing the entire RSJ circuit [Fig. 2(a)]. Both dc and ac bias currents or voltages can be applied. Values of resistances are in ohms unless noted otherwise. See text for further discussion of components.

lation, was no more than $\pm$ 2 parts in 10^5. These specifications were at least an order of magnitude better for the three AD 537's than for the several 4046's and one 8038 we tested, so we chose the AD 537. The excessive frequency drift of the other types leads to drifts of a few microamps in the current $I_c \sin\theta$ and corresponding drifts of several millivolts in the junction voltage $V(t)$. However, if cost is an overriding consideration the very inexpensive 4046 can be used.[25]

The sinusoidal reference oscillator also should have good drift and jitter characteristics. We have used an ancient, but excellent, Hewlett-Packard model 606A as our reference oscillator; its drift and jitter are somewhat smaller than those of the AD 537. We expect that any physics or electrical engineering department would own an oscillator of comparable quality.

The mixer must be capable of multiplying the sinusoidal output signal from the reference oscillator by the square-wave output of the AD 537, both of which are signals with frequency $\approx$ 100 kHz. We have tried an Analog Devices AD 532 JD integrated circuit multiplier, and also a CMOS-type 4052 multiplexer as a switching mixer, in which the reference oscillator signal and an inverted version of the oscillator signal are alternately connected to the input of the low-pass filter according to the polarity of the VCO output. While both devices are satisfactory as mixers, we chose the AD 532, despite its higher cost, because it does not require an inverted version of the reference oscillator signal. Because the linearity of the AD 532 multiplier begins to deteriorate for input signal amplitudes above 5 V we include a blocking capacitor and a 3-to-1 voltage divider between the $\pm$ 15-V VCO output and the multiplier input. This divider reduces the square-wave input signal to the multiplier from the VCO to approximately $\pm$ 5 V, with an average value of zero. The 0.1-μF coupling capacitor insures that the square-wave signal applied to the mixer has no dc component. This is necessary because the output resistance of the VCO is not the same for the positive and negative halves of the square wave, and the voltage divider loads the output slightly.

The low-pass filter following the mixer is a two-section passive RC filter, each section having a time constant τ of about 10 μsec or cut-off frequency of 16 kHz. This filter attenuates dc and low-frequency signals by approximately a factor of two, while it attenuates the second harmonic in the mixer output wave (near 200 kHz) by a factor of about $2\omega^2\tau^2 \approx 320$.

The mode switch between the low-pass filter and the op-amp input allows the overall feedback loop to be broken. When the switch is in the voltage bias (grounded) position and $C = 0$, the ac and dc bias voltages are multiplied by 1/5, added and inverted by the op-amp to produce the voltage $V(t)$. This corresponds to voltage biasing the supercurrent channel of a Josephson junction, rather than current biasing the junction as suggested by Fig. 2(a). For this voltage bias case the voltage $\sin\theta(t)$ at the filter output is the analog of the supercurrent $I_c \sin\theta(t)$. The voltage bias position of the mode switch is also used in setting the frequency of the reference oscillator (see Sec. V) and in checking for spurious frequency locking (Appendix A).

The circuit of Fig. 3 is powered by a commercial $\pm$ 15-V supply (e.g., Analog Devices 915). The circuit draws a supply current of about 15 mA. Only moderate care is required in laying out the circuit board. The leads to the 1000-pF VCO capacitor are kept short and the reference oscillator input is shielded all the way to the multiplier input in a coaxial cable. These precautions help to eliminate the spurious locking problem discussed in Appendix A. The entire circuit shown in Fig. 3 including the power supply was built inside a small aluminum box. This is strongly recommended, as it simplifies the setup and allows the student to concentrate on the terminal properties of the Josephson junction before having to master the details of the circuit. The aluminum box is connected to the power supply ground and acts as a shield. BNC connectors are used for signal inputs and outputs, and screw terminals on the front panel allow connection of different values of junction resistance (2.0 kΩ in our model) and junction capacitance. Resistor values are not critical, but 1% metal film resistors and a silver mica 1000-pF capacitor are used where indicated to insure temperature stability of the circuit. The junction capacitance C should be a high-quality monolithic or mylar capacitor. The 100-Ω, 33-μF decoupling filters must be included to avoid spurious frequency locking (see Appendix A), though the component values are not critical. The 1.5-kΩ resistor in the op-amp circuit helps to compensate for voltage offset due to the bias current of the 741 op-amp.[22] The signal current into the noninverting input is zero, so that this input is in fact at ground potential. Finally, the 20-kΩ trimpot permits adjustment of the multiplier output voltage to zero when its input voltages are zero.

IV. NORMALIZATION FACTORS FOR THE ANALOG

In order to make comparisons between voltages, currents, times, and capacitances of the analog, and voltages, currents, times, and capacitances of real Josephson junctions, it is useful to establish a set of units or normalization factors for the analog. Thus in agreement with other workers, we normalize currents to I_c, voltages to I_cR, times to $1/kI_cR$, and capacitances to $1/kI_cR^2$.

In our circuit $I_c = 100\,\mu$A, $k = 1.21\times10^4$ rad/V sec, and $R = 2000\,\Omega$. With this set of parameters the normalization factors for current, voltage, time and capacitance are shown in column 1 of Table I. Also shown in Table I are normalization factors in a typical real Josephson junction, with $I_c = 100\,\mu$A, $R = 10\,\Omega$, and

$$k = 2e/\hbar = 2\pi/\Phi_0 = 3.04\times10^{15} \text{ rad/V sec.}$$

Here Φ_0 is the superconducting flux quantum, $= 2.07\times10^{-15}$ V sec. The table shows, for example, that

Table I. Comparison of normalization factors for current, voltage, time, and capacitance, and junction parameters used to calculate these normalization factors, in the analog and in a typical real junction.

	Electronic analog	Real junction
Normalization factors		
Current I	100 μA	100 μA
Voltage V	200 mV	1 mV
Time t	0.41 msec	0.33 psec
Capacitance C	0.21 μF	0.033 pF
Junction parameters		
Resistance R	2 kΩ	10 Ω
Voltage-to-frequency conversion factor (rad/V sec)	$k = 1.21\times10^4$	$2e/\hbar = 3.04\times10^{15}$

the analog is more than 10^9 times slower than a typical real junction. Thus the analog can show, on a millisecond time scale, variations of voltages and currents that occur in a real junction on a picosecond time scale.

In describing regimes of behavior with $C \neq 0$, it is common to define a parameter[20] β_c, which is the normalized junction capacitance:

$$\beta_c = kI_cR^2C \equiv \omega_c\tau = (2e/\hbar)I_cR^2C,$$

where the second form applies for real junctions. The parameter ω_c is the characteristic angular frequency, kI_cR, and $\tau = RC$ is the damping time. For real junctions $\omega_c/2\pi$ is on the order of the energy gap frequency, $E_g/h \approx 10^{12}$ Hz. The normalized capacitance β_c determines the shape of the current–voltage curve and the amount of hysteresis (see Sec. V B).

V. OPERATION OF THE ANALOG AND TYPICAL RESULTS

Adjustment of the electronic analog prior to modeling is quite simple. After allowing the VCO and reference oscillator to warm up for a few minutes, and with the mode switch in the grounded position (voltage bias mode) and no dc or ac bias applied, one adjusts the reference oscillator frequency until the "beat frequency" of the voltage $\sin\theta$ observed on an oscilloscope is within 1 Hz or less of zero. This adjustment should be checked at frequent intervals. To obtain a critical current of 100 μA one adjusts the amplitude of the reference oscillator until the beats of $\sin\theta$ as observed on an oscilloscope are precisely $\pm$ 1.0 V in amplitude.

A. Voltage bias

As discussed earlier, when the mode switch is in the grounded (voltage bias) position and if $C = 0$, the dc or ac bias voltages produce a $V(t)$ across the VCO input given by $V(t) = \frac{1}{3}V_x = \frac{1}{3}(V_{dc} + V_{ac})$. The signal $\sin\theta$ then represents the supercurrent that flows in response to the changing phase difference produced by $V(t)$. If $V(t)$ is a dc voltage (i.e., $V_{ac} = 0$) then the phase difference changes at a constant rate and the supercurrent I_s (proportional to $\sin\theta$) is a *sinusoidal* function of time. This oscillation of I_s is called the Josephson oscillation; the frequency is $k\langle V(t)\rangle/2\pi = kV_{dc}/2\pi$.

If in addition to a dc voltage a sinusoidal voltage is applied to the junction, then the rate of change of phase, $d\theta/dt$, is modulated at a sinusoidal rate. In communications terminology this is called frequency modulation. An especially interesting case occurs if the dc voltage is adjusted to give a Josephson oscillation at the same frequency as that of the ac bias voltage. For example, denoting the bias voltage (dc + ac) as

$$V(t) = V_0 + V_1\cos 2\pi f_1 t, \tag{16}$$

we have from Eq. (13),

$$\frac{d\theta}{dt} = kV_0 + kV_1\cos 2\pi f_1 t. \tag{17}$$

Integrating, we obtain

$$\theta(t) = kV_0t + \theta_0 + (kV_1/2\pi f_1)\sin 2\pi f_1 t, \tag{18}$$

where θ_0 is a constant of integration. Equation (18) shows that the phase $\theta(t)$ changes by 2π in the time $T = 2\pi/kV_0$ provided V_0 is adjusted to equal $2\pi f_1/k$; in this case the supercurrent $I_c\sin\theta(t)$ has a well-defined average value. In practice it is impossible to adjust V_0 precisely; therefore the average value of $\sin\theta$ (over a few cycles) will slowly oscillate through a range of values on either side of zero. This short-term average of $\sin\theta$ has a maximum amplitude given by[16] $J_1(kV_1/2\pi f_1)$, where J_1 is the first-order Bessel function.[26] The slow oscillation of the maximum amplitude of $\sin\theta$ and the dependence of the maximum amplitude of $\sin\theta$ on V_1 are easily demonstrated quantitatively with the analog.

Nonzero average supercurrents can also be observed when V_0 is adjusted to give Josephson oscillations at 2, 3, etc. times the frequency of the applied ac bias voltage, i.e., $kV_0 = 2\pi nf_1$, with $n = 2$, 3, etc. The maximum average supercurrent for each of these dc voltages is given by $J_n(kV_1/2\pi f_1)$, with $n = 2$, 3, etc.

B. Current bias

Because of the necessity of running long wires into a Dewar, the high frequencies of the Josephson current oscillations ($\sim 10^{12}$ Hz) and the inductance of the long lead wires make it very difficult to voltage bias a real Josephson junction with a true ac voltage bias. (It is, as we have seen, straightforward to do this with the analog.) On the other hand, current bias is relatively easy to achieve for real junctions. The analog is quite useful in demonstrating the behavior of a junction under current bias conditions, especially for the case of simultaneous dc and ac current bias, for which an analytic solution has not been given.

An important special case that can be treated analytically occurs if $C = 0$ and only a dc bias current, I_0, is applied. Then Eq. (15) reduces to

$$I_0 = \frac{1}{kR}\frac{d\theta}{dt} + I_c\sin\theta \tag{19}$$

with $I_0 = V_x/R_x$. For $|I_0| < I_c$ the solution is $\theta = \sin^{-1}\times(I_0/I_c) = \text{const}$, so $d\theta/dt$ and V are both zero. (The circuit itself is acting as a phase-locked loop, with the phase θ automatically adjusted so that $V = 0$ despite the nonzero value of I_0.) If $|I_0|$ exceeds I_c then θ can no longer be constant and a time-varying voltage is developed across the junction. Still, Eq. (19) may be integrated directly (see Appendix B). Clearly, for positive values of $I_0 > I_c$, $d\theta/dt$ is always positive,and it is shown in Appendix B that its average value, $\langle d\theta/dt\rangle$, is $kR\sqrt{(I_0^2 - I_c^2)}$. From Eq. (2) and $k \rightarrow 2e/\hbar$ we find the time-average junction voltage:

$$\langle V\rangle = \frac{1}{k}\left\langle\frac{d\theta}{dt}\right\rangle = R\sqrt{(I_0^2 - I_c^2)}. \tag{20}$$

Brackets are used to denote averages with respect to time.

The analog can be used to trace out a curve of $\langle V\rangle$ as a function of I_0 on an x-y recorder.[27] One simply places the mode switch in the current bias position and connects the dc bias output terminal to one axis of the recorder and the time-average junction voltage $\langle V\rangle$ to the other. A plot of $\langle V\rangle$ as a function of I_0 appears in Fig. 4(a). The actual waveform of $\sin\theta$ as a function of time is shown, for three points on this I_0–$\langle V\rangle$ curve, in Fig. 5. Notice that as $\langle V\rangle$ increases the supercurrent oscillations have a higher fundamental frequency. This fundamental frequency, given by the Josephson relation, Eq. (2), is equal to $2e\langle V\rangle/h$. As $\langle V\rangle$ increases the supercurrent oscillations also become more sinusoidal. Consequently, the average value of the supercurrent approaches zero, and the I_0–$\langle V\rangle$ curve approaches

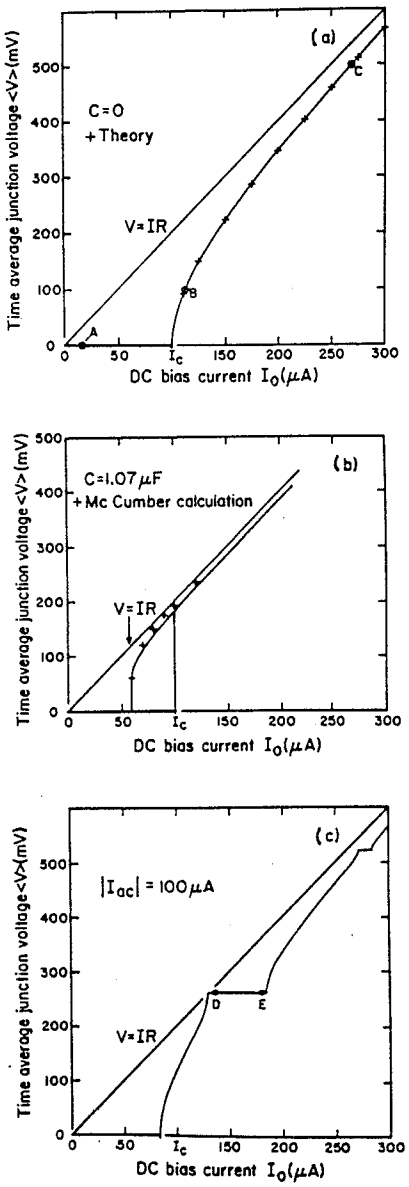

Fig. 4. Graphs of time average junction voltage $\langle V \rangle$ as a function of applied dc bias current I_0 obtained with the electronic analog of the RSJ circuit with $I_c = 100\ \mu A$ and $R = 2.00\ k\Omega$. (a) Junction capacitance $C = 0$, no ac bias current. For $C = 0$ the I–$\langle V \rangle$ curve is single valued. The crosses represent the predictions of Eq. (20). (b) Junction capacitance $= 1.07\ \mu F$ ($\beta_c = 5.2$), no ac bias current. As the current I_0 increases from below to above I_c, the junction voltage jumps to the upper curve. When I_0 is decreased the junction voltage is finite down to a lower current, $< I_c$. The I–$\langle V \rangle$ curve is thus hysteretic. The crosses are taken from computer calculations by McCumber, Ref. 20, for $\beta_c = 4$ and shown in his Fig. 4. Differences between our experimental result and McCumber's result are believed to be due primarily to effects of the low-pass filter circuit. (c) Junction capacitance $C = 0$. A sinusoidal ac bias current of $100\ \mu A$ zero-to-peak value at a frequency of 500 Hz was applied in addition to the variable dc bias current I_0. Constant voltage steps occur at voltages equal to integral multiples of ω_1/k, with ω_1 the ac angular frequency. The straight diagonal line in each graph is the I–V curve for the ohmic quasiparticle channel, $R = 2.00\ k\Omega$.

that of an ordinary resistor, $V = I_0R$, with $R = 2.0\ k\Omega$ for the circuit shown.

In taking the photo in Fig. 5 the camera shutter was open for several sweeps of the trace. It is evident in trace B that there is some jitter in the period of the Josephson oscillation. The fractional jitter is even worse for longer periods (I_0 more nearly equal to I_c). Since this jitter represents fluctuations in the time required for the VCO signal to slip by one cycle relative to the reference oscillator signal, any noise source that affects $d\theta/dt$ will contribute to this jitter. Such noise includes noise in the several resistors in the circuit, fluctuations in the amplitude or frequency of the reference oscillator, amplifier noise in the op-amp and mixer, and frequency jitter in the VCO.

If capacitance C is added in parallel across the terminals of the junction (between pins 2 and 6 of the op-amp), the I_0–$\langle V \rangle$ curve becomes hysteretic. That is, as the dc applied current I_0 is increased the junction voltage remains zero until I_0 exceeds I_c, at which point $d\theta/dt$ and V suddenly begin to oscillate with nonzero average values. So far this is qualitatively similar to the behavior with $C = 0$. But if I_0 is now reduced below I_c these oscillations continue until a lower critical current is reached. A typical hysteresis curve is shown in Fig. 4(b) for $C = 1.07\ \mu F$ (or $\beta_c = 5.2$). The lower critical current approaches zero as C is made larger. Hysteresis is predicted to occur for $\beta_c > 0.8$.[20,11] In phase-locked-loop terminology hysteresis corresponds to the lock range being greater than the capture range.

A second effect of parallel capacitance is to reduce the amplitude of the oscillating component of $V(t)$, and make it more sinusoidal. [To see this effect, one would current bias the junction at $I_0 \approx 1.5I_c$ and observe $V(t)$ on an oscilloscope for the two cases $C = 0$ and $C \approx 1\ \mu F$.] As a result, less time-average current is carried by the supercurrent channel. Furthermore, no dc current flows through the capacitor. Thus the I_0–$\langle V \rangle$ curve with finite capacitance is closer to the curve $\langle V \rangle = I_0R$ than when $C = 0$.

An important phenomenon, which confirms the second Josephson equation [Eq. (2)], occurs when sinusoidal current is applied in addition to dc current so that the total junction current $I(t) = I_{dc} + I_{ac} = I_0 + I_1 \cos 2\pi f_1 t$. Figure 4(c) shows an example for the special case $C = 0$. Here the dc current I_0 was varied and $\langle V \rangle$ plotted as a function of I_0 for a fixed amplitude of bias current $I_1 = V_{ac}/R_x$. Clearly evident are ranges of I_0 for which the average junction voltage is independent if I_0. These constant voltage steps, called Shapiro steps,[3] are separated by

$$\Delta \langle V \rangle = 2\pi f_1/k,$$

where f_1 is the frequency of the applied ac current. In a real junction $k = 2e/\hbar$ so a measurement of the step separation $\Delta \langle V \rangle$ and the applied (microwave) frequency f_1 yields a value of e/h. This kind of experiment has provided the best measurements[6] of e/h and of the fine-structure constant, and has led to the resolution of certain difficulties in quan-

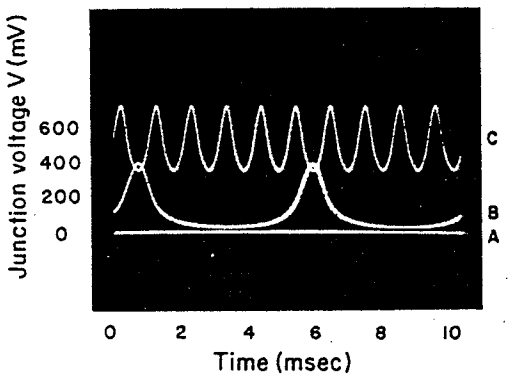

Fig. 5. Junction voltage plotted versus time for points A, B, and C of Fig. 4(a). Note the highly nonsinusoidal Josephson oscillations in B, where the dc bias current I_0 is only slightly larger than the critical current I_c. For each trace the camera shutter was open for ~ 0.1 sec and several sweeps were recorded. The slight jitter in the period of the Josephson oscillation that is evident in trace B is discussed in the text.

tum electrodynamics.[28]

As an aid in understanding why a range of dc applied currents can give the same average junction voltage, we show in Fig. 6 the time variation of junction voltage at two points D, E near either end of the first Shapiro step in Fig. 4(c). Both curves have the same fundamental frequency as the applied ac current, here 500 Hz, and therefore the same *average* voltage. Thus while the average current through R is the same at points D and E, the average supercurrent $\langle I_c \sin\theta \rangle$ must be larger at E than at D. The different $\sin\theta(t)$ waveforms at D and E can easily be displayed to demonstrate this effect.

The observation by Shapiro of these constant-voltage steps provided the first confirmation of the ac Josephson effect, Eq. (2), and a direct proof of the quantum nature of the superconducting ground state, since the absorption of a microwave photon of energy $E = \hbar\omega$ is required. The direct detection of photons at $\hbar\omega = 2\text{eV}$ emitted by a Josephson junction occurred somewhat later,[29] due to the difficulty of detecting the very small power emitted. The dc Josephson effect, i.e., the existence of a zero-voltage supercurrent, was confirmed[2] shortly after Josephson's prediction. However, it is only recently that direct measurements of the dependence of I_s on θ have been possible.[21] These measurements required the development of SQUID magnetometers, which themselves employ the Josephson effect.

C. Small signal behavior, with $I_0 < I_c$

If the junction is biased with a steady current I_0 less than I_c, while it is simultaneously driven by a small sinusoidal current, so that $I_s(t) = I_0 + I_1 \sin\omega_1 t$ with $I_1 \ll I_c$, then θ undergoes small oscillations about its equilibrium value, $\theta_{eq} = \sin^{-1}(I_0/I_c)$. This is easily seen by differentiating Eq. (1) to obtain

$$\frac{dI_s}{dt} = I_c \cos\theta \frac{d\theta}{dt} \approx I_c \cos\theta_{eq} \frac{d\theta}{dt}$$
$$= I_c(1 - \sin^2\theta_{eq})^{1/2} \frac{d\theta}{dt} = I_c[1 - (I_0/I_c)^2]^{1/2} \frac{d\theta}{dt}, \tag{21}$$

and then substituting for $d\theta/dt$ from Eq. (13) and rearranging, to arrive at

$$V(t) = \frac{1}{k(I_c^2 - I_0^2)^{1/2}} \frac{dI_s}{dt}. \tag{22}$$

Thus for small signals the supercurrent channel behaves like an inductor of value

$$L_J = 1/k(I_c^2 - I_0^2)^{1/2}. \tag{23}$$

The value of L_J in a real Josephson junction with $I_c = 100$ μA and $I_0 = 0$ is 3 pH. In our analog, with $k = 1.21 \times 10^4$ rad/V sec and $I_c = 100$ μA, this Josephson inductance is 0.83 H for $I_0 = 0$.

Because of the inductive behavior of the supercurrent channel, the entire Josephson junction acts as a parallel RLC circuit for small signals. We therefore expect a resonance of the junction voltage as we vary the frequency of an applied sinusoidal current of fixed amplitude. In the analog with a capacitance of 1.0 μF this resonance occurs at a frequency of approximately $f = 1/2\pi(L_J C)^{1/2} = 175$ Hz, which is easily observed by increasing R to about 20 kΩ in order to increase the Q of the resonant circuit. This so-called plasma resonance occurs at microwave frequencies or higher in real Josephson junctions. Note that this resonance frequency can be changed by changing the dc bias current I_0. The supercurrent channel thus behaves like a parametric inductor, which can lead to a variety of useful circuit applications.

VI. SIMULATION OF A JOSEPHSON COMPUTER ELEMENT

The application of Josephson junctions as sensitive analog detectors of magnetic fields, voltages, or high-frequency radiation has led to instruments that are the most sensitive currently available, and which approach the fundamental quantum noise limits.[30] The potential of Josephson junctions as ultrafast *digital* circuit elements has also been appreciated, starting with the pioneering work of Matisoo in the mid-1960s.[31] Prototype Josephson junction computer circuits are currently under study in a number of industrial laboratories, including IBM and Bell Laboratories. The type of device used in these applications is the oxide–barrier tunnel junction [Fig. 1(a)], which has a nonlinear quasiparticle conductance. In this section we discuss the qualitatively similar switching behavior of the RSJ circuit [Fig. 2(a)].

A useful figure of merit for switching elements used in computers is the product of the average power dissipation P in a single device times the delay time or switching time τ_D of the device. Small values of both P and τ_D are required for very fast computers. This is because, as τ_D itself is made smaller, the size of the computer must be reduced so that signal propagation times are also reduced. The density of circuit elements will thus increase, and heat removal from these circuit elements becomes a fundamental problem that can only be solved by reducing the power dissipation per device. Stated differently, if a short switching time is accompanied by high power dissipation, the allowable density of elements may be so low that propagation time, rather than the intrinsically smaller device switching time, may limit the speed of the computer. The $P\tau_D$ product for the semiconductor devices used in present computers is about 10^{-11} J. Switching devices made with Josephson junctions have achieved $P\tau_D$ products[32] of $\approx 10^{-16}$ J. Anacker[7] has recently described the design of a computer based on Josephson junction logic and memory elements, with circuit complexity roughly comparable to a current IBM Model 370/168 computer, which uses semiconductor devices.

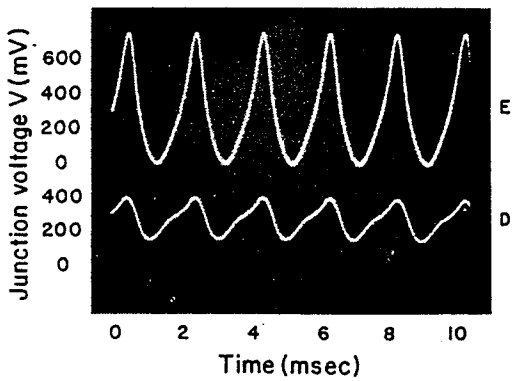

Fig. 6. Junction voltage plotted versus time for points D and E in Fig. 4(c), on the first Shapiro step. Both waves have the same fundamental frequency (500 Hz) as the ac bias current. As shown in Fig. 4(c), the time average voltages are the same for curves D and E, $\langle V \rangle = 260$ mV.

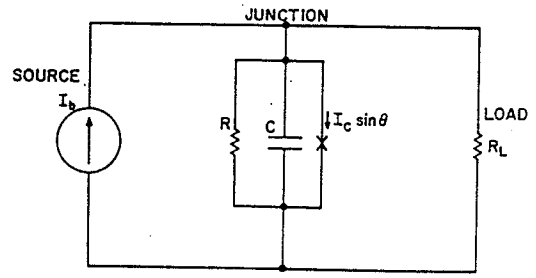

Fig. 7. Circuit model of an early form of Josephson computer switching element, the magnetic-field-switched, in-line gate. The junction is biased with a dc current I_b. In the zero-voltage state all of the bias current flows as supercurrent in the junction and none reaches the load R_L. In the voltage state some of the bias current flows through R_L. The junction is switched into the voltage state by application of a magnetic field, which decreases I_c. The current through R_L produces a magnetic field that can be used to switch another similar circuit.

The Josephson junction computer would have overall performance a factor of 20 times that of the 370/168 computer. The Josephson computer would have a machine cycle time 20 times faster than the 370/168, and a main memory 3 times larger with an access time also 20 times faster than the 370/168. The Josephson junction computer would dissipate 7 W at 4.2 K, and have a volume for the cooled electronics of $\approx 3\times 10^3$ cm^3, comparable to a desk-top calculator. Cryogenic cooling would of course be required.

The first type of Josephson switching element studied,[31] called an in-line gate, utilized the magnetic field dependence of the critical current of a single oxide–barrier tunnel junction. (See Matisoo, Ref. 7, p. 57 for a three-dimensional perspective of such a junction.) The effect of a magnetic field oriented with **B** perpendicular to the direction of current flow through the junction is to produce an additional phase shift $\theta(x)$ that varies with position x along the surface of the junction.[8] The supercurrent through the junction is given by

$$I_s = \int\int J_c \sin\theta(x) dA,$$

where J_c is the critical current density and A is the area. This integral implies interference between currents with different values of $\theta(x)$ [e.g., current with $\theta(x)=\pi/2$ through an area element is cancelled by that with $\theta(x)=-\pi/2$ through another area element.] The resulting expression for the maximum or critical supercurrent as a function of the magnetic flux is given in Ref. 8, and is like that for single-slit diffraction in optics.

In such a magnetic-field-dependent switching element the junction is biased with a dc current I_b, which is somewhat less than the critical current with no field, I_{c0}. Application of a magnetic field reduces the critical current to a new value $I_{c1} < I_b$. The junction will thus switch from a point on the I–$\langle V\rangle$ curve for the initial value of critical current, I_{c0}, to a point on the I–$\langle V\rangle$ curve for the new critical current I_{c1}. Figure 7 shows one possible biasing arrangement, in which a current source supplies dc current I_b to a Josephson junction in parallel with a load resistor R_L. In Fig. 8(a) we have drawn a load line, representing the effect of the external elements I_b and R_L, on the I–$\langle V\rangle$ characteristics for a junction with two different values of I_c, denoted by I_{c0} and I_{c1}. These I–$\langle V\rangle$ characteristics represent a resistively shunted junction [Fig. 2(a)] with negligible capacitance. (Such low-capacitance junctions have only recently been realized in practice with oxide–barrier tunnel junctions.)

Switching of the analog can be achieved by suddenly connecting a 200-kΩ resistor across the 49.9-kΩ input resistor of the multiplier with a pushbutton switch. The voltage across the 200-kΩ resistor can provide a triggering signal to the oscilloscope. Whenever $I_c = I_{c0}$ the circuit resides at point A in Fig. 8(a) and the voltage across R_L is zero; but when $I_c = I_{c1}$ the circuit resides at point B and there is a finite voltage across R_L.

In almost all oxide–barrier Josephson elements the capacitance is large enough to produce hysteresis [Fig. 8(b)]. For this case, if we begin with $I_c = I_{c0}$ and with the circuit at point C in Fig. 8(b), it switches to point D when I_c is reduced to I_{c1} and it remains at (i.e., latches at) point D after I_c returns to I_{c0}. To return the circuit to point C one must reduce the bias current briefly to zero. (Nonlatching logic is modeled by the $C=0$ case.)

Most Josephson devices under development as computer switching elements employ tunnel junctions, which have quasiparticle I–V characteristics like that shown in Fig. 8(b) as a dashed curve. With $\beta_c \gg 1$, a tunnel-junction gate

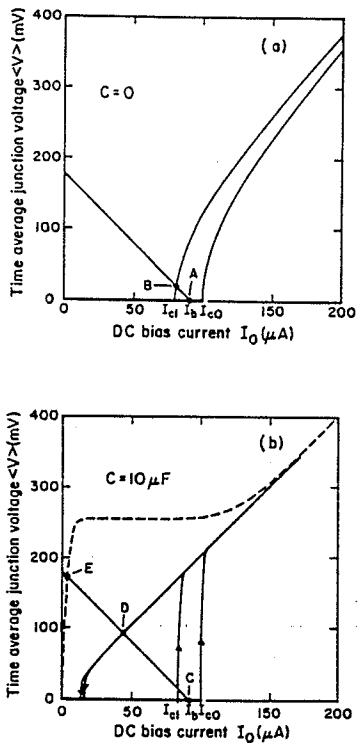

Fig. 8. Load lines are drawn on the I–$\langle V\rangle$ curves for a junction with two different values of critical current, I_{c0} and I_{c1}, to model a Josephson junction computer element, Fig. 7. In (a) the junction capacitance (and β_c) are zero and the I–$\langle V\rangle$ curve for each value of I_c is single valued. The junction switches from point A to point B when I_c is reduced to I_{c1}. In (b) the capacitance is 10 μF ($\beta_c \approx 50$) and the I–$\langle V\rangle$ curves are hysteretic. The junction switches from point C to point D when I_c is reduced to I_{c1}. The dashed curve in (b) represents a typical I–$\langle V\rangle$ curve for an insulator–barrier tunnel junction [see Fig. 1(a)]. This nonlinear quasiparticle characteristic is replaced by a straight line through the origin in the RSJ model. In practical in-line computer gates, insulator–barrier tunnel junctions with $\beta_c > 1$ are used and the I–$\langle V\rangle$ curve has two branches, one having $\langle V\rangle = 0$ and the other being almost exactly the quasiparticle curve. The switching then occurs between points C and E. To reset the gate and return to the zero-voltage state of point C, the bias current I_b must be reduced momentarily to near zero. Thus in-line gates with $\beta_c > 1$ are *latching* logic gates.

will switch from point C to point E upon application of a magnetic field.

Present designs of Josephson junction computers use multiple junction devices to form the basic logic (or memory) element. These include interferometers (SQUIDs) that can be switched by either a magnetic field[33] or by direct current injection,[32] and other multijunction structures.[34] All these devices allow *independent* variation of the inductance and critical current, thus giving much better performance and economy of space as lithographic dimensions are reduced, as compared with in-line junctions. Wider operating margins also can be achieved with current injection.[32]

Figure 9 shows an oscilloscope trace of junction voltage as a function of time, as the junction switches from point C to point D in Fig. 8(b), following a sudden reduction of the critical current from I_{c0} to I_{c1}. The Josephson oscillations are clearly visible on the switching waveform. After the initiation period of $\simeq 20$ msec, the waveform has a risetime of $\simeq R_{\|}C$, as expected from simple circuit theory if I_{c1} were zero. ($R_{\|}$ is the parallel combination of R and R_L, here equal to 1.0 kΩ.) Since I_{c1} is finite, Josephson oscillations are also clearly visible on the switching waveform. We find this combination of Josephson and RC times to be a beautiful demonstration of both the quantum-mechanical and the classical behavior of Josephson junction devices.

VII. CONCLUSIONS

We have shown that an electronic Josephson junction analog constructed from just three integrated circuits plus an external reference oscillator can exhibit many of the circuit phenomena of a real Josephson junction. The time scale for the electronic analog is more than 10^9 times slower than a real junction, permitting voltage and current waveforms to be displayed on an ordinary oscilloscope. The waveforms and I–V characteristics obtained from the analog give insight into the circuit behavior that cannot easily be obtained from the nonlinear differential equations that describe the Josephson junction.

ACKNOWLEDGMENTS

We wish to thank M. R. Beasley for valuable discussions of Josephson effect electronics, and A. Bliven for construction of an early version of the simulator circuit. An even earlier version of this circuit was employed in the Graduate Experimental Laboratory at Harvard University. This work was supported in part by NSF grants ENG-7710164 and ECS-7927165. Support of a sabbatical leave by Bucknell University to one of us (RWH) is also gratefully acknowledged.

APPENDIX A

When we first breadboarded a design similar to that of Fig. 3 we experienced a minor problem that proved to be difficult to troubleshoot because it came from two sources. The problem was manifested as Shapiro steps [see Fig. 4(c)] of nonzero slope, with the voltage at the end (E) of the first step being about 1% greater than the voltage at the beginning (D) of the step. This turned out to be caused by what we call spurious locking. Spurious locking is a tendency for the VCO to run at the same average frequency as the reference oscillator even when the $\sin\theta$ feedback to the VCO input through R_c is not present. The two causes of spurious locking were found to be (i) a direct interaction between the reference oscillator input and the VCO via the *sync* input (pin 2) of the AD 537 VCO and (ii) a less direct interaction between the multiplier and VCO via the power supply. The first problem was solved by shunting the VCO *sync* input to ground with a 0.1-μF capacitor and by using a grounded shield around the reference oscillator input lead. The second was solved by inserting 100-Ω, 33-μF decoupling filters in the power supply connections to the AD 532 multiplier and the AD 537 VCO.

In addition we found an easier method of detecting spurious locking than setting up simultaneous dc and ac current biasing and observing the slope of the Shapiro steps. All one need do is break the loop by setting the mode switch to the grounded, or voltage bias, position and observe the $\sin\theta$ waveform on an oscilloscope as the reference oscillator frequency is varied. With no spurious locking $\sin\theta$ should be a sinusoidal function of time even for very low (~ 1 Hz) difference frequencies. Spurious locking shows up as a nonsinusoidal (for example, a sawtooth) variation of $\sin\theta$ with time and, if the problem is really serious, the VCO frequency may even lock to the reference oscillator frequency.

APPENDIX B

Equation (20) relates the average junction voltage $\langle V \rangle$ to the dc bias current I_0 for the case of zero junction capacitance and $I_0 > I_c$. This result was first stated by Stewart and McCumber[20] and by Aslamazov and Larkin,[35] and is widely used in comparisons of experimental data with the predictions of the RSJ model. Solymar (Ref. 6; p. 167–9 and Appendix 6) has given derivations of the time-dependent quantities $V(t)$ and $I_s(t)$ using normalized variables. For completeness, and also to show explicitly the dependence on experimental variables, we present here an outline of a similar derivation.

To obtain Eq. (20) we begin with Eq. (19) and separate the variables to obtain

$$kR\,dt = d\theta/(I_0 - I_c \sin\theta). \tag{B1}$$

The indefinite integral of the right-hand side is given in standard tables, for example, Dwight[36] (No. 436.00) or *Handbook of Chemistry and Physics*, 51st ed.[37] (No. 340). The result of integrating Eq. (B1) is

$$kRt + \text{const} = \frac{2}{(I_0^2 - I_c^2)^{1/2}} \tan^{-1}\left(\frac{I_0 \tan(\theta/2) - I_c}{(I_0^2 - I_c^2)^{1/2}}\right). \tag{B2}$$

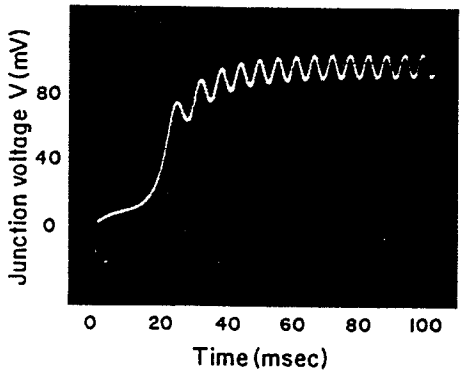

Fig. 9. Junction voltage as a function of time after the critical current is reduced from 100 μA to about 80 μA by connecting a 200-kΩ resistor in parallel with the 49.9-kΩ input resistor of the multiplier with a pushbutton switch. The junction capacitance is 10 μF as in Fig. 8(b).

It is convenient to choose the constant of integration to be

$$-\frac{2}{(I_0^2-I_c^2)^{1/2}}\tan^{-1}\left(\frac{I_0+I_c}{I_0-I_c}\right)^{1/2}$$

so that $\theta=-\pi/2$ at $t=0$. With this choice Eq. (B2) may be solved, after considerable manipulation, to give the explicit time dependences:

$$\sin\theta(t)=\frac{I_c-I_0\cos[kR(I_0^2-I_c^2)^{1/2}t]}{I_0-I_c\cos[kR(I_0^2-I_c^2)^{1/2}t]} \tag{B3}$$

and

$$V(t)=k^{-1}\frac{d\theta}{dt}$$
$$=\frac{R(I_0^2-I_c^2)}{I_0-I_c+2I_c\sin^2[(kR/2)(I_0^2-I_c^2)^{1/2}t]}. \tag{B4}$$

Equation (B4) agrees with Eq. (148) of Ref. 21 and with Eq. (6) of Ref. 35. It may be compared directly with curves like B and C in Fig. 5, and Eq. (B3) may be compared with the $\sin\theta(t)$ output of the analog.

The expressions for $\sin\theta(t)$ and $V(t)$ given in Eqs. (B3) and (B4) are seen to be periodic with period

$$T=2\pi/kR(I_0^2-I_c^2)^{1/2}. \tag{B5}$$

In order to compute the time average voltage $\langle V\rangle$, we take the time average value of both sides of Eq. (13). Clearly, the time average value of $d\theta/dt$ is $2\pi/T$, which we may write in terms of I_0 with the help of Eq. (B5). The result for $\langle V\rangle$ is

$$\langle V\rangle=k^{-1}\left\langle\frac{d\theta}{dt}\right\rangle=\frac{2\pi}{kT}=R(I_0^2-I_c^2)^{1/2}, \tag{B6}$$

which is Eq. (20) in the text.

Note added in proof. Recently two of the authors have developed a slightly different electronic analog based on a sample-and-hold technique applied to the reference oscillator signal.[15] That analog is somewhat simpler and less expensive, but does *not* provide as good an illustration of the mixing process and lock-in amplifier operation. However, if one wishes to emphasize only the junction terminal properties, then the other analog design[15] may be preferred. Our discussion applies in full for both analog circuits.

[a]Permanent address.

[1]B. D. Josephson, Rev. Mod. Phys. **36**, 216 (1964); Phys. Lett. **1**, 251 (1962).

[2]P. W. Anderson and J. M. Rowell, Phys. Rev. Lett. **10**, 230 (1963); J. M. Rowell, *ibid.* **11**, 200 (1963).

[3]S. Shapiro, Phys. Rev. Lett. **11**, 80 (1963).

[4]M. Tinkham, *Introduction to Superconductivity* (McGraw-Hill, New York, 1975).

[5]John Clarke, Proc. IEEE **61**, 8 (1973); Phys. Today **24** (8), 30 (1971); L. Solymar, *Superconductive Tunneling and Applications* (Chapman and Hall, London, 1972); A. Davidson, R. S. Newbower, and M. R. Beasley, Rev. Sci. Instrum. **45**, 838 (1974); Paul L. Richards, Franz Auracher, and Theodore Van Duzer, Proc. IEEE **61**, 36 (1973) discuss high-frequency detectors.

[6]T. F. Finnegan, A. Denenstein, and D. N. Langenberg, Phys. Rev. B **4**, 1487 (1971). A review of these experiments has been given by J. Clarke, Am. J. Phys. **38**, 1071 (1970).

[7]J. Matisoo, Sci. Am. **242** (5), 50 (1980); W. Anacker, IEEE Spectrum **16** (5), 26 (1979); IBM J. Res. Dev. **24**, (March 1980).

[8]A clear elementary derivation of the Josephson equations and quantum interference has been given by R. P. Feynman, R. B. Leighton, and M. Sands, *The Feynman Lectures on Physics* (Addison-Wesley, Reading, MA, 1965) Vol. III, Chap. 21. A similar discussion appears in C. Kittel, *Introduction to Solid State Physics*, 5th ed. (Wiley, New York, 1976), Chap. 12, and in Ref. 10. A nonmathematical discussion of quantum interference and the Josephson effects is given by D. N. Langenberg, D. J. Scalapino, and B. N. Taylor, Sci. Am. **224** (5), 30 (1966).

[9]D. B. Sullivan and J. E. Zimmerman, Am. J. Phys. **39**, 1504 (1971).

[10]G. I. Rochlin and P. K. Hansma, Am. J. Phys. **41**, 878 (1973). A very clear discussion of the various types of Josephson devices is given in this article.

[11]A comprehensive review of Josephson junction analogs has been given by T. A. Fulton, *Superconductor Applications: SQUIDS and Machines*, edited by Brian B. Schwartz and Simon Foner (Plenum, New York, 1977), Chap. 4. A short, clear discussion of the mechanical analog has been given by A. C. Rose-Innes and E. H. Rhoderick, *Introduction to Superconductivity*, 2nd ed. (Pergamon, New York, 1978), Chap. 11.

[12]D. B. Tuckerman, Rev. Sci. Instrum. **49**, 835 (1978); J. H. Magerlein, *ibid.* **49**, 486 (1978); A. Yagi and I. Kurosawa, *ibid.* **51**, 41 (1980).

[13]C. A. Hamilton, Rev. Sci. Instrum. **43**, 445 (1972); M. B. Simmonds and W. H. Parker, J. Appl. Phys. **42**, 38 (1971).

[14]C. K. Bak and N. F. Pederson, Appl. Phys. Lett. **22**, 149 (1973); C. K. Bak, Rev. Phys. Appl. **9**, 15 (1974).

[15]R. W. Henry and D. E. Prober, Rev. Sci. Instrum. **52**, 902 (1981), describe the use of similar junction analogs in simulation of single-junction and double-junction SQUIDs. Use of a junction analog to simulate the characteristics of an oxide-barrier tunnel junction (see Ref. 7) is described by D. E. Prober, S. E. G. Slusky, R. W. Henry, and L. D. Jackel, J. Appl. Phys. **52**, 4145 (1981).

[16]P. L. Richards, S. Shapiro, and C. C. Grimes, Am. J. Phys. **36**, 690 (1968).

[17]J. Bardeen, L. N. Cooper, and J. R. Schrieffer, Phys. Rev. **108**, 1175 (1957).

[18]We follow the rather standard convention that the electronic charge $q_e=e=-|e|$. (An exception to this convention is Kittel, Ref. 8.) As a result, certain of the resulting coefficients are implicitly negative. Another convention followed in this work is that the energies E_1 and E_2 are defined to include the effects of the Josephson coupling energy, which is proportional to $\cos\theta_0$.

[19]I. Giaever, Phys. Rev. Lett. **5**, 147 (1960).

[20]W. C. Stewart, Appl. Phys. Lett. **12**, 277 (1968); and D. E. McCumber, J. Appl. Phys. **39**, 3113 (1968). The RSJ model neglects interaction between the pair and quasiparticle currents. This interaction introduces an additional term in Eq. (3), which is proportional to $\cos\theta$. This term is usually neglected, as its effects are small; see Ref. 4, p. 195; also, Ref. 21, p. 140.

[21]K. K. Likharev, Rev. Mod. Phys. **51**, 101 (1979).

[22]R. W. Henry, *Electronic Systems and Instrumentation* (Wiley, New York, 1978), Chap. 8.

[23]The virtual ground approximation is discussed in many places, for example, Ref. 22, Chap. 8; W. G. Oldham and S. E. Schwarz, *An Introduction to Electronics* (Holt, Rinehart and Winston, New York, 1972), Chap. 12; and R. E. Simpson, *Introductory Electronics for Scientists and Engineers* (Allyn and Bacon, Boston, MA, 1974), Chap. 9.

[24]Analog Devices, Inc., Norwood, MA 02062.

[25]RCA COS/MOS Integrated Circuits Handbook (1977), pp. 475 and 612.

[26]*Handbook of Mathematical Functions*, edited by M. Abramowitz and I. Stegun (Dover, New York, 1965), Chap. 9.

[27]Hewlett Packard, Model 7047A *x-y* recorder. Hewlett-Packard, Palo Alto, CA 94304.

[28]B. N. Taylor, W. H. Parker, and D. N. Langenberg, Rev. Mod. Phys. **41**, 375 (1969); see also Ref. 6.

[29]D. N. Langenberg, D. J. Scalapino, B. N. Taylor, and R. E. Eck, Phys. Rev. Lett. **15**, 294 (1965); I. M. Dmitrenko and I. K. Yanson, Sov. Phys. JETP **22**, 1190 (1965).

[30]Mark B. Ketchen and Richard F. Voss, Appl. Phys. Lett. **35**, 812 (1979).

[31]J. Matisoo, Proc. IEEE **55**, 172 (1967).

[32]T. R. Gheewala, Appl. Phys. Lett. **34**, 670 (1979); S. M. Faris, IBM Tech. Discl. Bull. **20**, 2031 (1977).

[33]H. Zappe, IEEE Trans. Magn. **13**, 41 (1977).

[34]T. A. Fulton, S. S. Pei, and L. N. Dunkleberger, Appl. Phys. Lett. **34**, 709 (1979).
[35]L. G. Aslamazov and A. I. Larkin, JETP Lett. **9**, 87 (1969).
[36]H. B. Dwight, *Tables of Integrals and Other Mathematical Data*, revised ed. (Macmillan, New York, 1947).
[37]*Handbook of Chemistry and Physics*, 51st ed. (Chemical Rubber, Cleveland, OH, 1970).

 0002-9505/81/111046-05$00.50